Journal of Coordination Chemistry
Publication details, including instructions for authors and subscription information:
http://www.tandfonline.com/loi/gcoo20

DNA interaction and cytotoxicity studies of ruthenium(III) complexes containing 3-(benzothiazol-2-yliminomethyl)-naphthalen-2-ol ligand

Subbaiyan Sathiyaraj [a], Ray J. Butcher [b] & Chinnasamy Jayabalakrishnan [a]

[a] Post Graduate and Research Department of Chemistry, Sri Ramakrishna Mission Vidyalaya College of Arts and Science, Coimbatore, India

[b] Department of Chemistry, Howard University, Washington, DC, USA

Accepted author version posted online: 17 Jan 2013.Published online: 25 Feb 2013.

To cite this article: Subbaiyan Sathiyaraj, Ray J. Butcher & Chinnasamy Jayabalakrishnan (2013) DNA interaction and cytotoxicity studies of ruthenium(III) complexes containing 3-(benzothiazol-2-yliminomethyl)-naphthalen-2-ol ligand, Journal of Coordination Chemistry, 66:4, 580-591, DOI: 10.1080/00958972.2013.764995

To link to this article: http://dx.doi.org/10.1080/00958972.2013.764995

Journal of Coordination Chemistry
Vol. 66, No. 4, 20 February 2013, 580–591

DNA interaction and cytotoxicity studies of ruthenium(III) complexes containing 3-(benzothiazol-2-yliminomethyl)-naphthalen-2-ol ligand

SUBBAIYAN SATHIYARAJ†, RAY J. BUTCHER‡ and CHINNASAMY JAYABALAKRISHNAN*†

†Post Graduate and Research Department of Chemistry, Sri Ramakrishna Mission Vidyalaya College of Arts and Science, Coimbatore, India
‡Department of Chemistry, Howard University, Washington, DC, USA

(*Received 8 June 2012; in final form 11 October 2012*)

A new Schiff base, 3-(benzothiazol-2-yliminomethyl)-naphthalen-2-ol, has been synthesized and characterized by elemental analysis, Fourier transform infrared spectroscopy (FT-IR), UV–vis, nuclear magnetic resonance, and single-crystal X-ray diffraction. Ruthenium(III) complexes of the Schiff base were synthesized and characterized by analytical and spectroscopic (FT-IR, UV–vis, and electron paramagnetic resonance) data as well as magnetic susceptibility measurements. DNA-binding properties of the ligand and its ruthenium(III) complexes have been investigated by electronic absorption spectroscopy. The three ruthenium(III) complexes were tested for DNA cleavage. Further *in vitro* study of the cytotoxity of the ligand and the complexes on human cervical cancer cell line and human laryngeal epithelial carcinoma cell line were carried out.

Keywords: Ruthenium(III) complexes; Crystal structure; DNA-interaction; Cytotoxicity

1. Introduction

Metal complexes that can interact with DNA have been studied as DNA footprint, novel chemotherapeutics, and highly sensitive diagnostic agents [1–6]. Transition metals play a very important role in organisms, and their complexes can interact non-covalently with nucleic acid by intercalation, groove-binding or external electrostatic binding [3,7–11]. Many transition metal complexes have been investigated as probes of DNA structure, agents for mediation of strand scission of duplex DNA and chemotherapeutic agents [12–14]. Some Pt(II) complexes (cisplatin and carboplatin) have found their way into pharmaceutical use as clinical antitumor drugs [15]. Schiff bases show a variety of biological actions by virtue of the azomethine linkage, which is responsible for various antibacterial, antifungal, herbicidal, and clinical activities [16–18]. Polyfunctional ligands based on benzazole derivatives, such as 2-aminobenzothiazole, 2-aminothiazole, and 2-aminobenzoxazole have biological activity as fungicides, antibiotics, pesticides, and neuroprotectors [19–21]. Thiazole derivatives are widely used in the synthesis of medical products such as sulfathiazole [22].

*Corresponding author. Email: srkvmca@md4.vsnl.net.in

Journal of Coordination Chemistry
ISSN 0095-8972 print/ISSN 1029-0389 online © 2013 Taylor & Francis
http://dx.doi.org/10.1080/00958972.2013.764995

A large number of ruthenium Schiff base complexes have been reported and their catalytic and biological properties studied [23–29]. Intercalation, hydrogen bonding, and π–π interactions are implicated in the mode of action of ruthenium complexes as antitumor and antimetastatic agents. Ruthenium–halogen bonds in several ruthenium complexes exhibiting anticancer activity suggest that these bonds may also play an important role. Herein, we report the synthesis and characterization of a new Schiff base derived from the condensation of 2-aminobenzothiazole with 2-hydroxy-1-naphthaldehyde and its ruthenium(III) complexes. DNA binding and cleavage behaviors were examined using UV spectroscopic and gel electrophoresis techniques, respectively, and cytotoxic abilities of ruthenium(III) complexes were examined using 3-(4,5-dimethylthiazol-2-yl)-2,5-diphenyl tetrazolium bromide (MTT) assay. The Schiff base was structurally characterized by single-crystal X-ray diffraction.

2. Experimental

2.1. *Materials and instrumentation*

Reagent grade chemicals were used without purification in all the synthetic work. All solvents were purified by standard methods. 2-Hydroxy-1-naphthaldehyde and 2-amino benzothiazole were purchased from Sigma-Aldrich. $RuCl_3{\cdot}3H_2O$, triphenylphosphine/arsine was purchased from Himedia. $[RuCl_3(PPh_3)_3]$ [30], $[RuCl_3(AsPh_3)_3]$ [31], and $[RuBr_3(PPh_3)_3]$ [32] were prepared by reported methods. Calf-thymus DNA (CT-DNA) was purchased from Bangalore Genei, Bangalore, India. The human cervical cancer cell line (HeLa) and human laryngeal epithelial carcinoma cell line (HEp2) were obtained from the NCCS, Pune, India.

Infrared spectra were recorded on a FT-IR Perkin Elmer spectrophotometer RXI model as KBr pellets from 4000 to 400 cm^{-1}. Elemental analyzes were performed with a Vario ELIII CHNS at the Sophisticated Test and Instrumentation Center (STIC), Cochin University, Kerala. Electronic spectra were recorded in dimethylsulfoxide (DMSO) solution in a Systronics 2202 double-beam spectrophotometer from 800 to 200 nm. ^1H and ^{13}C spectra were recorded on a Bruker WM DCX 500 MHz instrument using TMS as an internal standard at SAIF, Indian Institute of Technology, Chennai. Magnetic susceptibility measurements of the complexes were recorded using a Guoy balance at room temperature. X-band electron paramagnetic resonance spectra of the complexes were recorded on a Varian E-112 spectrometer using TCNE as the standard at the SAIF, Indian Institute of Technology Bombay, Mumbai, India. DNA cleavage studies were carried out using Gelstan, Gel documentation system. Anticancer studies were carried out at the Kovai Medical Center and Hospital Pharmacy College, Coimbatore, Tamilnadu. Melting points were recorded with a Veego DS model apparatus and are uncorrected.

2.2. *Crystal structure determination*

Single crystal of the Schiff base (HL) was obtained by slow solvent evaporation of the ligand in chloroform. Selected crystal data are given in tables 2 and 3. The X-ray diffraction data for HL were collected on a Bruker SMART CCD diffractometer using graphite-monochromated Mo Kα radiation ($\lambda = 0.71073$ Å) by ϕ and ω scans. X-ray data reduction

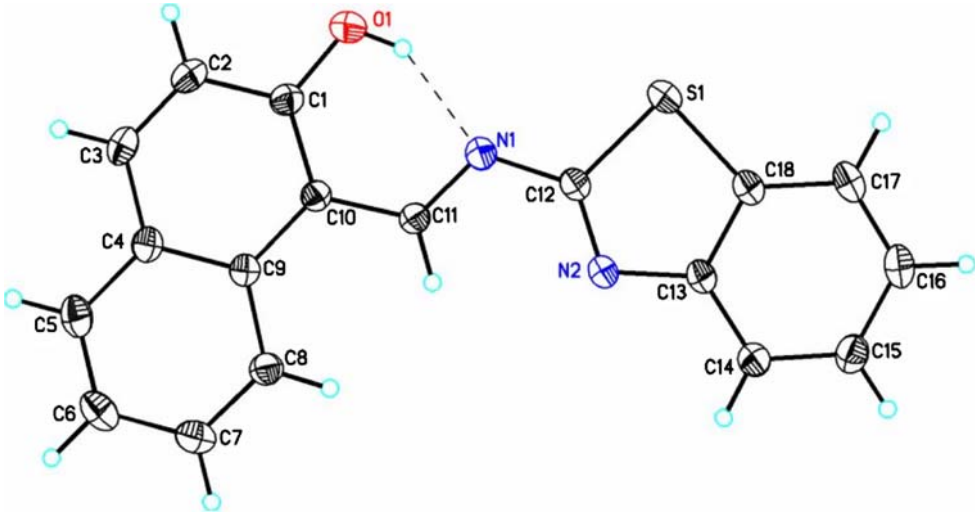

Figure 1. Labeled ORTEP diagram of HL with thermal ellipsoid at 50% probaility.

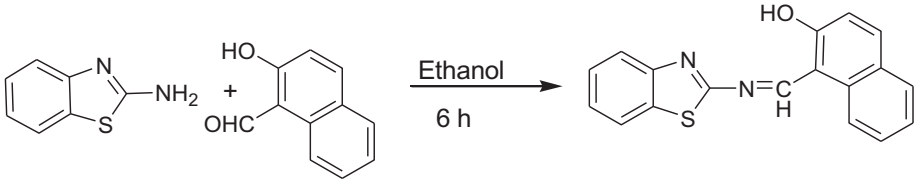

Scheme 1. Formation of Schiff base ligand.

structure solution and refinement were done using the SHELXS-97 and SHELXL-97 packages [33]. The structure (figure 1) was solved by direct methods.

2.3. *Synthesis of the Schiff base ligand*

3-(Benzothiazol-2-yliminomethyl)-naphthalen-2-ol (HL) was isolated from condensation of 2-hydroxy-1-naphthaldehyde (1.20 g, 10 mmol) and 2-amino benzothiazole (1.5 g, 10 mmol) in ethanol under reflux for 6 h. After cooling the reaction mixture to room temperature, the solid product formed was filtered, washed with ethanol and dried *in vacuo* (scheme 1). Purity was checked by TLC. This solid was recrystallized from chloroform, yielding orange crystals suitable for X-ray diffraction analysis.

2.4. *Synthesis of ruthenium(III) Schiff base complexes*

The new ruthenium complexes were prepared by the following general procedure (scheme 2). To a solution of $[RuX_3(EPh_3)_3]$ (0.1 mmol) in benzene (X = Cl/Br, E = PPh_3/$AsPh_3$) HL (0.1 mmol) in chloroform was added and the mixture was refluxed for 6 h. The solvent was then evaporated under reduced pressure and the solid mass filtered and washed with petroleum ether. The purity was checked by TLC and subjected to purification by column

chromatography. This solid was recrystallized from CH_2Cl_2/n-hexane mixture. Our efforts to obtain single crystals of the complexes were not successful.

2.5. *DNA-binding and cleavage assay*

2.5.1. Electronic absorption spectroscopy. Electronic absorption titration of the ligand and its complexes were carried out in aqueous buffer solution (50 mm NaCl, 5 mM Tris-HCl, pH 7.1) at fixed complex concentration (10 μM) while gradually increasing the concentration of CT-DNA. Absorption data were analyzed to evaluate the intrinsic binding constant K_b, which can be determined from the following equation [34]:

$$[\mathrm{DNA}]/(\varepsilon_a - \varepsilon_f) = [\mathrm{DNA}]/(\varepsilon_b - \varepsilon_f) + 1/K_b(\varepsilon_b - \varepsilon_f)$$

where [DNA] is the concentration of DNA in base pairs, the apparent absorption coefficient ε_a, ε_f and ε_b correspond to A_{obsd}/[complex], the extinction coefficient of the free compound and the extinction coefficient of the compound when fully bound to DNA, respectively. In plots of [DNA] / $(\varepsilon_a - \varepsilon_f)$ versus [DNA], K_b is given by the ratio of slope to intercept.

2.5.2. DNA cleavage studies. Cleavage experiments of supercoiled pBR322 DNA (1 μg) in 5 mM Tris-HCl, 50 mM NaCl, buffer at pH 7.1, were carried out using agarose gel electrophoresis. The samples were incubated for 2 h at 37 °C. A loading buffer containing 25% bromophenol blue, 0.25% xylene cyanol, and 60% glycerol was added and electrophoresis was carried out at 50 V for 2 h in tris-acetic acid/ethylenediaminetetraacetic acid (EDTA) buffer using 1% agarose gel containing 1.0 μg/mL ethidium bromide. The bands were visualized under UV light and photographed. The cleavage efficiency was measured by determining the ability of the complex to convert supercoiled DNA (SC) to nicked circular form (NC) and linear form (LC).

2.6. *Cytotoxicity assay*

The human cervical cancer cell line (HeLa) and human laryngeal epithelial carcinoma cell line (HEp2) were obtained from the National Center for Cell Science (NCCS), Pune and grown in Eagles Minimum Essential Medium containing 10% fetal bovine serum (FBS). All cells were maintained at 37 °C, 5% CO_2, 95% air, and 100% relative humidity. Maintenance cultures were passaged weekly, and the culture medium was changed twice a week.

The monolayer cells were detached with trypsin-EDTA to make single-cell suspensions and viable cells were counted using a hemocytometer and diluted with medium with 5% FBS to give final density of 1×10^5 cells/mL. One hundred microliters per well of cell suspension were seeded into 96-well plates at plating density of 10,000 cells/well and incubated to allow for cell attachment at 37 °C, 5% CO_2, 95% air, and 100% relative humidity. After 24 h, the cells were treated with serial concentrations of the extracts and fractions. They were initially dissolved in neat DMSO and further diluted in serum-free medium to produce various concentrations. One hundred microliters per well of each concentration was added to plates to obtain final concentrations of 1.0, 0.5, 0.25, 0.125,

and 0.063 μg/mL. The final volume in each well was 200 μL, and the plates were incubated at 37 °C, 5% CO_2, 95% air, and 100% relative humidity for 48 h. The medium without samples served as control. Triplicates were maintained for all concentrations.

MTT is a yellow water-soluble tetrazolium salt. A mitochondrial enzyme in living cells, succinate-dehydrogenase, cleaves the tetrazolium ring, converting the MTT to an insoluble purple formazan. Therefore, the amount of formazan produced is directly proportional to the number of viable cells.

After 48 h of incubation, 15 μL of MTT (5 mg/mL) in phosphate-buffered saline was added to each well and incubated at 37 °C for 4 h. The medium with MTT was then flicked off, and the formed formazan crystals were solubilized in 100 μL of DMSO; the absorbance at 570 nm was measured using a microplate reader. The % cell inhibition was determined using the following formula.

$$\% \text{ Growth inhibition} = 100 - \text{Abs (sample)}/\text{Abs (control)} \times 100$$

A non-linear regression graph was plotted between % cell inhibition and $\log_{10}$ concentration, and IC_{50} was determined using Graph Pad Prism software [35,36].

3. Results and discussion

Three air stable, mononuclear octahedral ruthenium(III) Schiff base complexes, $[RuX_2(EPh_3)L]$ (where X = Cl or Br; E = P or As; L = monobasic tridentate Schiff base), have been prepared by reaction of $[RuX_3(EPh_3)_3]$ with HL in 1 : 1 M ratio in chloroform–benzene mixture. The analytical data (table 1) for the new complexes agree well with the proposed molecular formulas (scheme 2).

3.1. *Crystal structure of 3-(benzothiazol-2-yliminomethyl)-naphthalen-2-ol (HL)*

The molecular structure of HL along with the atom numbering-scheme is given in figure 1. The crystal data and structural refinement parameters are given in table 2 and selected bond lengths and angles are given in table 3. The compound crystallized into a monoclinic lattice with space group *P 21/n*. The azomethine bond, C12–N1 1.3943(19) Å, is in conformity with a formal C=N double bond, and the C1–O1 bond distance of 1.3348(18) Å is slightly shorter than the normal C–O single-bond distance. The bond distance for C12–N2 1.2941 (19) Å and C12–S1 1.7462(14) Å for thiazole are close to C–N and C–S single bonds. This compound exits in imine-ol form without any ambiguity.

Table 1. Analytical data of ligand and ruthenium(III) complexes.

Ligand and complexes	Color	Yield (%)	Melting point (°C)	Elemental analysis calculated (found)			
				C%	H%	N%	S%
HL	Orange	72	148	70.02 (70.30)	4.61 (4.33)	9.15 (8.92)	10.46 (10.12)
$[RuCl_2(PPh_3)L]$	Brown	62	170	58.62 (58.37)	3.55 (3.69)	3.80 (3.75)	4.35 (4.09)
$[RuCl_2(AsPh_3)L]$	Brown	67	158	55.32 (55.09)	3.35 (3.61)	3.58 (3.89)	4.10 (3.89)
$[RuBr_2(PPh_3)L]$	Dark brown	64	145	52.31 (52.62)	3.17 (3.38)	3.39 (3.11)	3.38 (3.53)

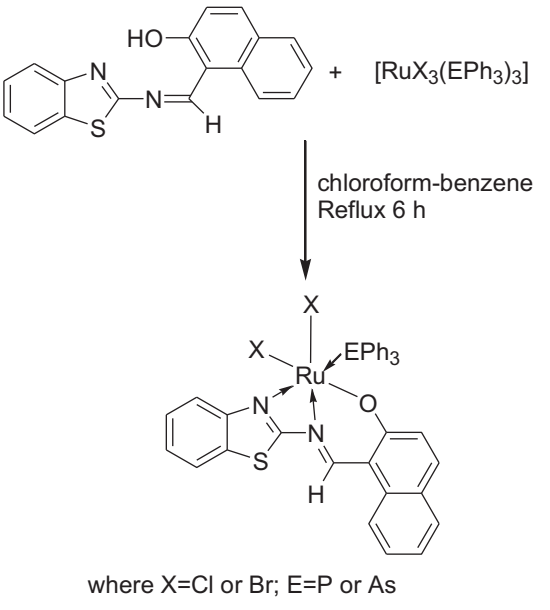

Scheme 2. Formation of ruthenium(III) Schiff base complexes.

Table 2. Crystal and structure refinement data for HL.

Empirical formula	$C_{18}H_{12}N_2OS$
Formula weight	304.36
Temperature	295(2) K
Wavelength	0.71073 Å
Crystal system	Monoclinic
Space group	P 21/n
Unit cell dimensions	
a (Å)	9.7176(3)
b (Å)	15.0806(6)
c (Å)	9.7882(3)
α (°)	90
β (°)	101.713(3)
γ (°)	90
Volume	1404.56(8) Å^3
Z	4
Density (calculated)	1.439 Mg/m^3
Crystal size	$0.47 \times 0.38 \times 0.24$ mm^3
Theta range for data collection	5.13–34.98°
Index ranges	$-15 \leqslant h \leqslant 14$, $-19 \leqslant k \leqslant 24$, $-15 \leqslant l \leqslant 14$
Reflections collected	12,583
Independent reflections	5739 [R(int) = 0.0261]
Refinement method	Full-matrix least-squares on F^2
Data/restraints/parameters	5739/0/200
Goodness-of-fit on F^2	1.035
Final R indices [$I > 2\sigma(I)$]	$R_1 = 0.0557$, $wR_2 = 0.1303$
R indices (all data)	$R_1 = 0.0956$, $wR_2 = 0.1518$
Largest diff. peak and hole	0.353 and -0.243 e Å^{-3}

Table 3. Selected bond lengths (Å) and angles (°) for HL.

Bond lengths		Bond angles	
S(1)–C(18)	1.7332(16)	C(18)–S(1)–C(12)	88.78(7)
S(1)–C(12)	1.7462(14)	C(1)–O(1)–H(1A)	109.5
O(1)–C(1)	1.3348(18)	C(11)–N(1)–C(12)	117.79(12)
O(1)–H(1A)	0.8200	C(12)–N(2)–C(13)	110.50(12)
N(1)–C(11)	1.3023(18)	O(1)–C(1)–C(10)	122.51(13)
N(1)–C(12)	1.3943(19)	O(1)–C(1)–C(2)	116.80(13)
N(2)–C(12)	1.2941(19)	C(10)–C(1)–C(2)	120.69(14)
N(2)–C(13)	1.3870(18)	C(3)–C(2)–C(1)	120.06(15)
C(1)–C(10)	1.406(2)	C(3)–C(2)–H(2A)	120.0
C(1)–C(2)	1.412(2)	C(1)–C(2)–H(2A)	120.0
C(2)–C(3)	1.353(2)	C(2)–C(3)–C(4)	122.15(14)
C(2)–H(2A)	0.9300	C(2)–C(3)–H(3A)	118.9
C(3)–C(4)	1.422(2)	C(4)–C(3)–H(3A)	118.9
C(3)–H(3A)	0.9300	C(5)–C(4)–C(9)	119.99(14)
C(4)–C(5)	1.408(2)	C(5)–C(4)–C(3)	121.16(14)
C(4)–C(9)	1.418(2)		

3.2. *Spectral characterization*

3.2.1. Infrared spectra. IR spectral data of the ligand were compared with those of the ruthenium(III) complexes to confirm the binding mode of HL to ruthenium and values are listed in table 4. HL has the most characteristic bands at 3396 cm^{-1} ν(O–H), 1622 cm^{-1} ν(C=N azomethine), 1599 cm^{-1} ν(C=N thiazole ring), 1311 cm^{-1} ν(Ph–CO), and 744 cm^{-1} ν(C–S–C). The band at 1622 cm^{-1} due to ν(C=N) underwent a shift to lower frequency (1601–1598 cm^{-1}) after complexation, indicating bonding of unsaturated nitrogen of the azomethine to ruthenium [37]. The phenolic C–O stretch that appeared at 1311 cm^{-1} in the ligand [38] shifts to higher frequencies (1340–1338 cm^{-1}) in the complexes. This shift confirms participation of oxygen in C–O–M bond. The low frequency at 430–470 cm^{-1} is attributed to (M–O) and 560–580 cm^{-1} to (M–N) [39]. IR spectrum of the ligand revealed a medium band at 1599 cm^{-1} for C=N of the thiazole ring, which shifts to lower frequency at 1586–1580 cm^{-1} after complexation, also indicating coordination to ruthenium. The unchanged band after complexation at 748 cm^{-1} for ν(C–S–C) in the free ligand suggests non-involvement of sulfur in coordination. Other characteristic bands due to triphenylphosphine/arsine were also present in the expected region [40].

Table 4. IR and electronic spectroscopic data of ligand and ruthenium(III) complexes.

	FT-IR cm^{-1}				UV–Vis
Ligand and complexes	ν(C=N)	ν(Ph-OH)	ν(Ph-CO)	ν(C=N) thiazole	λ_{max}, nm (ε, dm^3 mol^{-1} cm^{-1})
HL	1622	3396	1311	1598	276(1301), 365(1516), 445(2046), 476(2117)
$[RuCl_2(PPh_3)L]$	1601	–	1338	1586	256(1302), 297(1259), 364(1362), 409(1469), 438(1417), 520(701)
$[RuCl_2(AsPh_3)L]$	1598	–	1340	1583	256(1300), 301(1274), 363(1361), 405(1306), 432(1412), 524(693)
$[RuBr_2(PPh_3)L]$	1597	–	1338	1581	255(1280), 289(1226), 368(1469), 416(1900), 526(899)

3.2.2. Electronic spectra. Electronic spectra of HL and its complexes were recorded in DMSO (table 4) and are given in Supplementary material. Two very strong bands at 365 and 276 nm were observed in the spectrum of the ligand, attributed to n–π^* and π–π^* transitions in the aromatic ring and C=N [41]. These peaks shift in spectra of the complexes. Electronic spectra of all the complexes show four to five bands at 263–526 nm and their assignments are given in table 4. The ground state of ruthenium(III) (t_{2g}^5 configuration) is $^2T_{2g}$, while the first excited doublet levels in the order of increasing energy are $^2A_{2g}$ and $^2T_{1g}$, arising from the $t_{2g}{}^4\ e_g{}^1$ configuration [42]. In most ruthenium(III) complexes, electronic spectra show only charge transfer bands [43]. In a d^5 system, and especially in ruthenium(III) that has relatively high-oxidizing properties, charge transfer bands $L_{\pi y} \rightarrow t_{2g}$ are prominent in the low-energy region obscuring weaker d–d transitions. Therefore, it becomes difficult to assign conclusively the bands of ruthenium(III) complexes appearing in the visible region. Hence, all bands in this region have been assigned to charge transfer transitions, in conformity with assignments made for similar ruthenium(III) complexes [44–46].

3.2.3. ^{1}H and ^{13}C NMR spectra of the Schiff base. The formation of HL was monitored by peak ratios in the ^{1}H and ^{13}C NMR spectra recorded in DMSO-d_6 (Supplementary material). The aromatic proton for the ligand is a multiplet at 7.24–8.27 ppm. The proton of the hydroxyl group is a broad singlet at 10.12 (Ph–OH) ppm for free HL. The signal due to azomethine (–HC=N) is a singlet at 8.72 ppm. ^{13}C NMR spectrum of the Schiff base displays a single resonance at 152 ppm [47] which shows that the azomethine carbons are equivalent and also confirms the structure of the ligand. The signal at 166 ppm corresponds to the thiazolic C=N [48]. The resonance observed at 119–138 ppm is assigned to phenyl.

3.2.4. Magnetic moment and EPR spectra. The room temperature magnetic susceptibility measurements of the ruthenium(III) complexes showed that they are paramagnetic (μ_{eff} = 1.85–1.96 BM) with a single unpaired electron in a low-spin $4d^5$ configuration and confirms that ruthenium is in the +3 oxidation state.

The X-band EPR spectra of powdered samples of the complexes were recorded at room temperature and the "g" values are listed in table 5. The EPR experiments provide only the absolute "g" values and so neither their signs nor the correspondence of g_1, g_2 or g_3 to g_x, g_y or g_z are known. All the complexes exhibited $g_\perp$ at 2.49, 2.37, and 2.40 and $g_\parallel$ at 2.24, 2.23 and 2.23 (table 5 and Supplementary material). The two different "g" values ($g_x = g_y \neq g_z$) indicate a tetragonal distortion in these octahedral complexes. The presence of

Table 5. EPR and magnetic moment data of ruthenium(III) complexes.

Complexes	g_x	g_y	g_z	$\langle g \rangle^*$	μ_{eff} (BM)
$[RuCl_2(PPh_3)L]$	2.49	2.49	2.24	2.41	1.85
$[RuCl_2(AsPh_3)L]$	2.37	2.37	2.23	2.32	1.88
$[RuBr_2(PPh_3)L]$	2.40	2.40	2.23	2.34	1.96

$\langle g \rangle^* = [1/3g_x^2 + 1/3g_y^2 + 1/3g_z^2]^{1/2}$.

two "g" values also indicates axial symmetry. The nature and position of the lines in the spectra of the complexes are similar to those of octahedral complexes [53].

3.3. *DNA binding and cleavage*

3.3.1. Electronic absorption spectroscopy. Transition metal centers are particularly attractive moieties for the development of effective chemotherapeutic agents since they exhibit well-defined coordination geometries and also often possess distinctive electrochemical or photo-physical properties, thus enhancing the functionality of the binding agent [3]. The Schiff base and its complexes in DMSO-buffer mixture exhibit an intense transition at 252–260 nm, attributed to the π–π^* transition that is unique to this Schiff base. The binding of HL and complexes to the DNA helix have been characterized through absorption spectral titrations by following changes in absorbance and shift in wavelength. Figure 2 shows absorption spectra of ligand and ruthenium(III) complexes in the absence and presence of CT-DNA. Addition of increasing amounts of CT-DNA result in hyperchromism and blue shift. As the DNA-double helix possesses many hydrogen-bonding sites, it is likely that amine groups of the amino acid chain form hydrogen bonds with DNA, which may contribute to the hyperchromism observed. A similar hyperchromism has been observed also for a ruthenium(III) complex bearing a Schiff base ligand [54].

Intrinsic binding constants (K_b) were calculated for HL and ruthenium(III) complexes, 1.4×10^4 M^{-1} [HL], 2.9×10^4 M^{-1} [$RuCl_2(PPh_3)L$], 1.9×10^4 M^{-1} [$RuCl_2(AsPh_3)L$], 2.2×10^4 M^{-1} [$RuBr_2(PPh_3)L$]. The different DNA-binding affinity of the three ruthenium (III) complexes results from different co-ligands affecting binding affinity with DNA. K_b

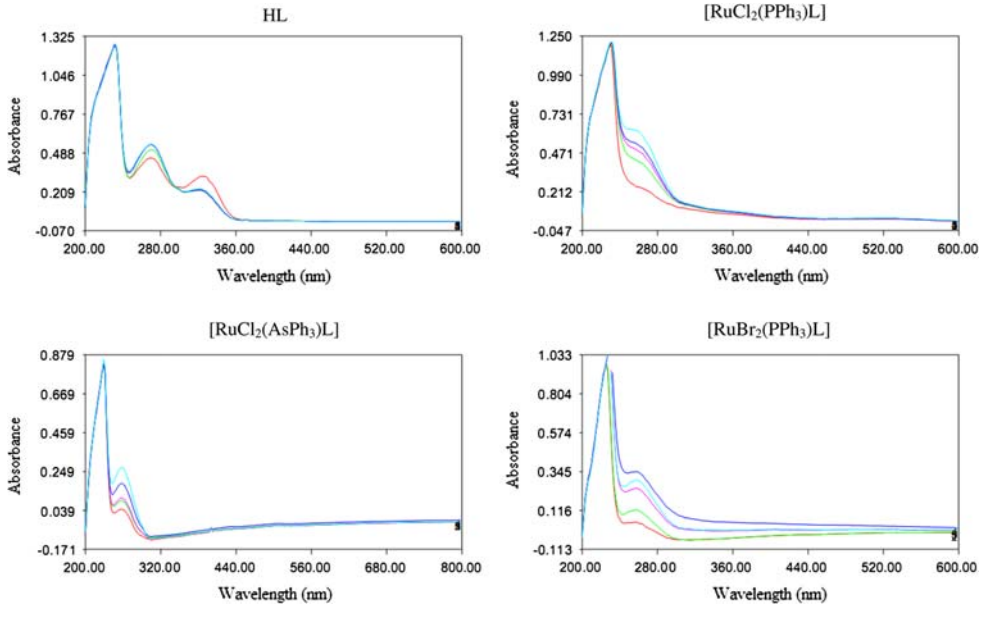

Figure 2. Absorption spectral traces of HL, [$RuCl_2(PPh_3)L$], [$RuCl_2(AsPh_3)L$] and [$RuBr_2(PPh_3)L$] with increasing concentration of CT-DNA in a Tris HCl-NaCl buffer (pH 7.1).

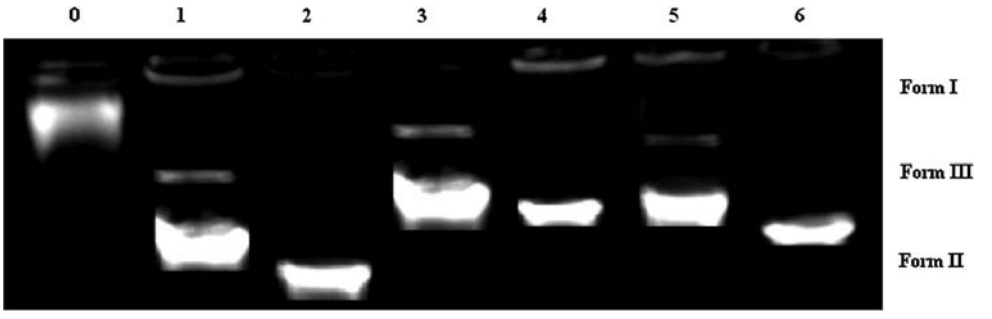

Figure 3. Gel electrophoresis showing the chemical nuclease activity of pBR322 plasmid DNA (1 μg) with different concentrations of the complexes; Lane 0: DNA control; Lane 1: 30 μM $[RuCl_2(PPh_3)L]$ + DNA; Lane 2: 60 μM $[RuCl_2(PPh_3)L]$ + DNA; Lane 3: 30 μM $[RuCl_2(AsPh_3)L]$ + DNA; Lane 4: 60 μM $[RuCl_2(AsPh_3)L]$ + DNA; Lane 5: 30 μM $[RuBr_2(PPh_3)L]$ + DNA; Lane 6: 60 μM $[RuBr_2(PPh_3)L]$ + DNA.

values obtained for the above ruthenium(III) complexes are comparable with those for $[Ru(dmp)_2(APIP)]^{2+}$ (APIP = 2-(2-aminophenyl)imidazo[4,5-f][1,10]phenanthroline), $2.3–3.3 \times 10^4\ M^{-1}$ [55].

3.3.2. Cleavage of pBR322 DNA by ruthenium(III) complexes. The ability of ruthenium(III) complexes to perform DNA cleavage is monitored by agarose gel electrophoresis and the pBR322 plasmid DNA is involved. Agarose gel electrophoresis is shown in figure 3. No DNA cleavage was observed for the control in which the metal complex was absent (lane 0), The relatively fast migration is the intact supercoil form (Form I) and the slower moving migration is the open circular form (Form II), which was generated from supercoiled when scission occurred on one strand [56,57]. With increasing concentration of the ruthenium(III) complexes (lanes 1 and 2 for $[RuCl_2(PPh_3)L]$, 3 and 4 for $[RuCl_2(AsPh_3)L]$ and 5 and 6 for $[RuBr_2(PPh_3)L]$), the amount of Form I of pBR322 DNA diminished gradually and the amount of the nicked circular DNA (Form II) increased remarkably. When the concentration increased to 60 μM for all the complexes, DNA was completely converted from Form I to Form II. $[RuCl_2(PPh_3)L]$ exhibits greater cleavage efficiency than other complexes which can be attributed to the longer metal to ligand charge transfer excited state lifetime of $[RuCl_2(PPh_3)L]$.

3.4. *Cytotoxic activity evaluation*

To test the cytotoxicity of Schiff base ligand and ruthenium(III) complexes, HeLa and HEp2 were cultured in the presence of varying concentrations of ligand and the corresponding ruthenium(III) complexes for 48 h. The inhibitory concentration 50 (IC_{50}) is defined as the concentration required to reduce the size of the cell population by 50%. The IC_{50} values of the ligand ($IC_{50} = 175$ μM) exhibit enhanced activity against HeLa cell line and low activity ($IC_{50} = 389$ μM) against HEp2. The IC_{50} values for the complex are 105, 212 μM for $[RuCl_2(PPh_3)L]$, 153, 275 μM for $[RuCl_2(AsPh_3)L]$ and 123, 323 μM for $[RuBr_2(PPh_3)L]$ against HeLa and HEp2 cell lines, respectively. All ruthenium(III) complexes show moderate activity against the two tumor cell lines. Thus, the IC_{50} value

for the ligand decreases with the coordination of it to ruthenium metal, which shows the higher toxicity of the complex than the ligand. Even though they possess better cytotoxicity, they could not reach the effectiveness of the standard drug cisplatin [58].

4. Conclusion

Three mononuclear ruthenium(III) Schiff base complexes were synthesized and characterized by various physico-chemical and spectroscopic methods, showing octahedral geometry. The binding of the ligand and the complexes with CT-DNA were tested using absorption titration studies with binding affinity in the order $[RuCl_2(PPh_3)L]$ > $[RuBr_2(PPh_3)L]$ > $[RuCl_2(AsPh_3)L]$ > HL. K_b values obtained for the above ruthenium(III) complexes are comparable than those for $[Ru(dmp)_2(APIP)]^{2+}$ (APIP = 2-(2-aminophenyl) imidazo[4,5-f][1,10]phenanthroline), $2.3–3.3 \times 10^4$ M^{-1} [55]. The DNA cleavage results showed that $[RuCl_2(PPh_3)L]$ has more cleavage activity than the other complexes. *In vitro* study of the cytotoxicity of the ligand and complexes on HeLa and HEp2 show moderate antitumor activity against selected cell lines.

Supplementary material

Crystallographic data for the structural analysis have been deposited with the Cambridge Crystallographic Data Center, CCDC 814145. Copy of this information may be obtained free of charge from the Director, CCDC, 12 Union Road, Cambridge, CB21 EZ, UK (Fax: +44 1223 36033: Email: deposit@ccdc.cam.ac.uk or www.ccdc.cam.ac.uk/deposit).

Acknowledgements

We sincerely thank University Grants Commission (UGC), New Delhi for financial support [Scheme No. 38-222/2009 (SR)]. One of the authors, RJB, wishes to acknowledge the NSF-MRI program (Grant No. CHE-0619278) for providing funds to purchase the diffractometer.

References

[1] A.M. Pyle, J.K. Barton. *Prog. Inorg. Chem.*, **38**, 413 (1990).
[2] T.D. Tullius. In *Metal–DNA Chemistry*, Ed. ACS Symposium Series, ACS, pp. 1–23, Washington, DC. 402, 1 (1989).
[3] C. Metcalfe, J.A. Thomas. *Chem. Soc. Rev.*, **32**, 215 (2003).
[4] K.E. Erkklia, D.T. Odom, J.K. Barton. *Chem. Rev.*, **99**, 2777 (1999).
[5] F. Liang, P. Wang, X. Zhou, T. Li, Z.Y. Li, H.K. Lin, D.Z. Gao, C.Y. Zheng, C.T. Wu. *Bioorg. Med. Chem. Lett.*, **14**, 1901 (2004).
[6] K. Jiao, Q.X. Wang, W. Sun, F.F. Jian. *J. Inorg. Biochem.*, **99**, 1369 (2005).
[7] A. Silvestri, G. Barone, G. Ruisi, M.T. Lo Giudice, S. Tumminello. *J. Inorg. Biochem.*, **98**, 589 (2004).
[8] C. Hemmert, M. Pitié, M. Renz, H. Gornitzka, S. Soulet, B. Meunier. *J. Biol. Inorg. Chem.*, **6**, 14 (2001).
[9] B. Macias, M.V. Villa, E. Fiz, I. Garcia, A. Castineiras, M.G. Alvarez, J. Borras. *J. Inorg. Biochem.*, **88**, 101 (2002).
[10] H. Zhang, C.S. Liu, X.H. Bu, M. Yang. *J. Inorg. Biochem.*, **99**, 1119 (2005).

[11] S. Sharma, S.K. Singh, M. Chandra, D.S. Pandey. *J. Inorg. Biochem.*, **99**, 458 (2005).
[12] N. Saglam, A. Colak, S. Dulaer, S. Guner, S. Karabocek, A.O. Belduz. *BioMetals*, **15**, 357 (2002).
[13] V. Uma, M. Kanthimathi, T. Weyhermuller, B.U. Nair. *J. Inorg. Biochem.*, **99**, 2299 (2005).
[14] Z.D. Xu, H. Liu, S.L. Xiao, M. Yang, X.H. Bu. *J. Inorg. Biochem.*, **90**, 79 (2002).
[15] C. Orvig, M.J. Abrams. *Chem. Rev.*, **99**, 2201 (1999).
[16] H.F. Abd El-halim, M.M. Omar, G.G. Mohamed. *Spectrochim. Acta, Part A*, **78**, 36 (2011).
[17] T.B.S.A. Ravoof, K.A. Crouse, M.I.M. Tahir, F.N.F. How, R. Rosli, D.J. Watkins. *Transition Met. Chem.*, **35**, 871 (2010).
[18] N. Padma Priya, S. Arunachalam, A. Manimaran, D. Muthupriya, C. Jayabalakrishnan. *Spectrochim. Acta, Part A*, **72**, 6706 (2009).
[19] C. Ramalingan, S. Balasubramanian, S. Kabilan, M. Vasudevan. *Eur. J. Med. Chem.*, **39**, 527 (2004).
[20] G.T. Zitouni, S. Demirayak, A. Ozdemir, Z.A. Kaplancikli, M.T. Yildiz. *Eur. J. Med. Chem.*, **39**, 267 (2004).
[21] M.A. Neelakantan, S.S. Marriappan, J. Dharmaraja, T. Jeyakumar, K. Muthukumaran. *Spectrochim. Acta, Part A*, **71**, 628 (2008).
[22] V.E. Borisenko, A. Koll, E.E. Kolmaov, A.G. Rjasnyi. *J. Mol. Struct.*, **783**, 101 (2006).
[23] P. Govindaswamy, Y.A. Mozharivskyj, M.R. Kollipara. *Polyhedron*, **23**, 1567 (2004).
[24] R.K. Rath, M. Nethaji, A.R. Chakravarty. *Polyhedron*, **21**, 1929 (2002).
[25] R.I. Kureshy, N.H. Khan, S.H.R. Abdi, S.T. Patel, P. Iyer. *J. Mol. Catal. A*, **150**, 163 (1999).
[26] P. Munshi, R. Samanta, G.K. Lahiri. *J. Organomet. Chem.*, **586**, 176 (1999).
[27] M.G. Bhowon, H.L.K. Wah, R. Narain. *Polyhedron*, **18**, 341 (1998).
[28] D.L. Davies, J. Fawcett, R. Krafczyk, D.R. Russell. *J. Organomet. Chem.*, **545**, 581 (1997).
[29] Z. Shirin, R.N. Mukherjee. *Polyhedron*, **11**, 2625 (1992).
[30] J. Chatt, G.J. Leigh, D.M.P. Mingos, R.J. Paske. *J. Chem. Soc. A*, 2636 (1968).
[31] R.K. Poddar, I.P. Khullar, U. Agarwala. *Inorg. Nucl. Chem. Lett.*, **10**, 221 (1974).
[32] K. Natarajan, R.K. Poddar, U. Agarwala. *J. Inorg. Nucl. Chem.*, **39**, 431 (1977).
[33] G.M. Sheldrick. *SHELXS -97, SHELXL-97 Fortran Programs for Crystal Structure Solution and Refinement*, University of Gottingen, Gottingen (1997).
[34] A. Wolfe, G.H. Shimer, Jr., T. Meehan. *Biochemistry*, **26**, 6392 (1987).
[35] T. Mosmann. *J. Immunol. Methods*, **65**, 55 (1983).
[36] A. Monks. *J. Nat. Cancer Inst.*, **83**, 757 (1991).
[37] R. Ramesh, M. Sivagamasundari. *Synth. React. Inorg. Met. Org. Chem.*, **33**, 899 (2003).
[38] R.C. Maurya, P. Patel, S. Rajput. *Synth. React. Inorg. Met. Org. Chem.*, **23**, 817 (2003).
[39] K. Nakamoto. *Infrared and Raman Spectra of Inorganic and Coordination Compounds*, Wiley Interscience, New York, NY (1971).
[40] A.K. Das, S.M. Peng, S.J. Bhattacharya. *Chem. Soc. Jpn*, **49**, 287 (1976).
[41] R.K. Sharma, R.V. Singh, J.P.J. Tandon. *Inorg. Nucl. Chem.*, **42**, 1382 (1980).
[42] C.J. Ballhausen. *Ligand Field Theory*, McGraw Hill, New York, NY (1962).
[43] A.B.P. Lever, *Inorganic Electronic Spectroscopy*, 2nd Edn., Elsevier, Amsterdam (1984).
[44] T.D. Thangadurai, K. Natarajan. *Indian J. Chem., Sect. A*, **40A**, 573 (2001).
[45] C. Jayabalakrishnan, R. Karvembu, K. Natarajan. *Synth. React. Inorg. Met. Org. Chem.*, **32**, 1101 (2002).
[46] A. Kumar Das, S-M. Perg, S. Bhattarcharya. *J. Chem. Soc., Dalton Trans.*, 181 (2000).
[47] J.T. Desai, C.K. Desai, K.R.I. Desai. *Iran. Chem. Soc.*, **5**, 67 (2008).
[48] S. Pérez, C. López, A. Caubet, X. Solans, M. Font-Bardía, M. Gich, E. Molins. *J. Organomet. Chem.*, **692**, 2402 (2007).
[49] A.K. Mahaparta, S. Datta, S. Goswami, M. Mukherjee, A.K. Mukherjee, A. Chakravorty. *Inorg. Chem.*, **25**, 1715 (1986).
[50] P. Ghosh, A. Pramanik, N. Bag, G.K. Lahiri, A. Chakravorty. *J. Organomet. Chem.*, **454**, 237 (1993).
[51] P. Munshi, R. Samanta, G.K. Lahiri. *Polyhedron*, **17**, 1913 (1998).
[52] G.K. Lahiri, S. Bhattacharya, M. Mukherjee, A.K. Mukherjee, A. Chakravorty. *Inorg. Chem.*, **26**, 3359 (1987).
[53] D. Bhattacharyya, S. Chakraborty, P. Munshi, G.K. Lahiri. *Polyhedron*, **18**, 2951 (1999).
[54] G. Raja, R.J. Butcher, C. Jayabalakrishnan. *Transition Met. Chem.*, **37**, 169 (2012).
[55] Z.H. Liang, Z.Z. Li, H.L. Huang, Y.J. Liu. *J. Coord. Chem.*, **64**, 3342 (2011).
[56] A.K. Parta, S. Dhar, M. Nethaji, A.R. Chakravarty. *Dalton Trans.*, 896 (2005).
[57] E. Gao, Y. Sun, Q. Liu, L. Duan. *J. Coord. Chem.*, **59**, 1295 (2006).
[58] Y.-J. Liu, C.-H. Zeng, Z.-H. Liang, J.-H. Yao, H.-L. Huang, Z.-Z. Li, F.-H. Eur. *J. Med. Chem.*, **45**, 3087 (2010).